ESR IN PULSED FIELDS

J. Witters and F. Herlach

Katholieke Universiteit Leuven
Celestijnenlaan 200 D
Leuven Belgium

Contents

I. Introduction

Very strong magnetic fields are needed to study magnetic resonances that are broadened by impurities, lattice deformation or other interactions such as the exchange energy in antiferromagnets. Certain phenomena that can be studied by means of magnetic resonances will occur only at very high magnetic fields, such as magnetic field induced phase transitions in the crystal lattice or in the arrangement of the electrons. The study of field-dependent effects over a broader field range may also call for very strong fields.

It is of course most convenient to do experiments in d.c. fields where the signal-to-noise ratio can be greatly improved by lock-in techniques. Fields up to 15 T are now conveniently available from superconducting coils; for higher sweep rates water-cooled high power coils are available at the large magnet laboratories. The highest d.c. fields now available are of the order of 30 T; these are generated by combining a 10 MW watercooled magnet with a large superconducting coil. Higher fields can only be obtained in a pulsed mode, as it will be discussed in section II of this paper, together with an overview of existing pulsed field installations.

For magnetic fields in the range 10 T - 100 T, a typical resonance frequency such as the Zeeman doublet with a free-electron g-factor of 2 is in the frequency range from 300 GHz to 3 THz (wavenumber range 10 cm^{-1} to 100 cm^{-1}), thus in the region from mm-waves into the far infrared. This frequency range is just between microwaves which can be transmitted through waveguides and light which can be focused by lenses; this requires the development of different experimental techniques. There are convenient sources of radiation such as the optically pumped far infrared laser for most of the frequency range, in particular the higher frequencies, and carcinotrons or IMPATT diodes for the lower frequencies. Regarding sensitive detectors, this frequency range presents some difficulty. It is too low for efficient photon detectors and on the high side for coherent detection techniques (heterodyne); there is certainly still much room for further development. This will be discussed in section III.

Different electron spin resonance (ESR) experiments have been performed in pulsed fields; among these the antiferromagnetic resonances (AFMR) are most prominent. This is quite natural since in many

antiferromagnets the zero field transition is in the FIR region (typically 30 cm^{-1}) and splits into two branches as a function of the field strength. Pulsed fields are sufficiently strong to break up the antiparallel alignment of the spins and to cause a phase transition to the paramagnetic state. Several interesting studies of AFMR spectra and of magnetic field induced phase transitions will be reported in section IV.

Electron resonances in the paramagnetic state (EPR) and in the ferromagnetic state (FMR) are not so common in the far infrared. Indeed, the advantage of FIR resonances in pulsed fields over microwave resonances in static fields is not so obvious at first sight. It appears that only in a few selected cases there is a real advantage in increasing the resonance field. However, it is expected that with the development of the technique more experiments will be extended to the high field regime, if only to follow up the magnetic field dependence of several parameters. Research of this kind will be discussed in section V, including some recent experiments.

II. Pulsed Magnetic Fields

With water-cooled coils, 15 T can be generated in a 5 cm bore with 5 MW and $\approx$ 20 T with 10 MW (Herlach, 1985). This enormous power must not only be provided and regulated – ideally with a stability of 10^{-5} – it must also be removed from the coil by a stream of water of the order of 100 liters per second. In a pulsed magnet, Joule heat is absorbed by the heat capacity of the coil and the power supply is an energy storage device such as a capacitor bank, a flywheel or an inductor. In exceptional cases, pulsed power of the order 10 MW can be obtained directly from the mains, with power conditioning by thyristors and passive filters (Gersdorf et al., 1965). The most common type of power supply is a capacitor bank with a typical energy of 100 kJ and peak voltage in the range 3 – 10 kV for fields < 100 T and up to 40 kV for fields > 100 T. Exceptionally, capacitor banks up to 1 MJ are used for obtaining a longer pulse duration. The design of a suitable pulsed power supply is well within the state of the art of modern electrical engineering. In particular, the technology of high power semiconductor switching devices is now in rapid development and provides excellent devices for power conditioning.

The most severe problem in generating magnetic fields in excess of 20 – 30 T is given by the magnetic stress. This amounts to 1 GPa (gigapascal) at 50 T, 4 GPa at 100 T and 100 GPa = 1 Mbar at 500 T = 5 megagauss. The energy density expressed in kJ/cm^3 is equal to the pressure in GPa. Given the fact that the strongest construction materials such as maraging steel have an ultimate tensile strength of the order of 2 GPa, it is evident that magnetic fields of more than 100 T cannot be contained in a stable mechanical structure. On basis of this criterion, pulsed magnetic fields can be divided loosely into three categories: "nondestructive" fields below 60 T with a relatively long pulse duration (10 ms - 1 s) determined by the energy stored in the power supply which must be matched by the heat capacity of the coil, "megagauss" fields > 100 T where destruction is inevitable and the pulse duration ($<5\mu s$) is limited by the propagation of shock waves through the confining structure, and finally a "gray" region between 60 T and 100 T where attempts are made to design nondestructive coils with partial inertial confinement and the pulse duration is of the order of 0.1 ms.

The mechanics of a nondestructive coil is similar to that of a vessel containing high pressure. However, by contrast to hydrostatic pressure which is applied only at the inner wall of the vessel, the magnetic force is distributed throughout the volume of the coil. The magnetic stress is proportional to the product of the current density which is constant in a wire-wound coil, and the magnetic field which decreases almost linearly from the inner to the outer radius. Although the magnetic stress is a decreasing function of the radius, the outer layers have a tendency for greater expansion because the total force exerted on a layer of the coil is proportional to the radius. This results easily in a negative radial stress whereby the outer layers of the coil exert a pull on the inner layers. Even a modest negative radial stress has the effect of strongly increasing the tangential stress at the inner radius (Witters and Herlach, 1983). A wire-wound coil consists of alternate layers of insulating and conducting material. This results in a complicated, inhomogeneous mechanical system. Therefore it is not feasible to make exact predictions of the mechanical behavior under extreme magnetic stress which will drive the inner layers into the limit of plastic deformation (Herlach et al., 1984). The relative softness of the insulating material attenuates the transmission of radial

stress. Therefore, a reasonable estimate of the peak field that can be supported by a wire-wound coil is given by the equation for the peak stress in a coil with free-standing windings:

$$B_{max} = 2(1 - 1/\alpha)\sqrt{\mu_0 \sigma} \qquad (1)$$

where α is the ratio of the outer and the inner radius, σ the ultimate tensile strength and $\mu_0 = 4\pi 10^{-7}$ Vs/Am.

The electrical resistance of the coil increases during the field pulse due to ohmic heating. This has a strong influence on the pulse shape and on the peak field, in particular for pulses of long duration. Precooling of the coil to liquid nitrogen temperature not only increases the amount of heat that can be absorbed by the coil without damage to the insulation, it is essential in decreasing the resistance to allow the flow of high current for a given supply voltage. Examples of computer simulations are given in Table I. In practice, most coils are wound from copper wire with rectangular cross section to obtain a good filling factor and to avoid slipping of the wires against each other. For additional containment, the coils are potted in epoxy and tightly enclosed in a high strength cylinder. The highest fields up to 60 T have been obtained with wire that incorporates a large number of fine niobium strands in a copper matrix (Ozhogin et al., 1983; Foner, 1986). This type of wire was originally developed for the manufacture of superconducting coils; in pulsed field coils it is not used in its superconducting state but only for its mechanical strength.

A wire-wound coil connected to a capacitor bank of 100 – 200 kJ is an elegant and compact laboratory instrument. Most modern capacitor banks for this application are switched by high power thyristors (typical performance data are 4 kV, 25 kA single shot per thyristor with the possibility of series and parallel connection), some with trigger generators using fiber optics. At voltage reversal the discharge is crowbarred by means of diodes with damping resistors. Thyristor switching is very smooth and reliable; the diode crowbar provides for a modest extension of the pulse duration and protects the capacitors from voltage reversal which would shorten their life expectation.

Table II is a listing of laboratories where nondestructive pulsed fields are presently available for research. Many of these accomodate guest experiments on the basis of mutual collaboration, in particular those at M.I.T., Osaka, Tokyo, Toulouse and Leuven. It is not really feasible to run a pulsed field laboratory as a general user's facility in the style of the big national d.c. magnet laboratories. Experimentation with pulsed fields requires much experience and special experimental techniques which are developed by the in-house research staff. The Osaka laboratory is different from most others in that this facility has been set up with the goal of generating 100 T nondestructively. The coils consist of two or three concentric solid helices machined from maraging steel and designed for optimal sharing of the total magnetic force. The low inductance of these coils results in a short pulse duration of the order 0.1 ms. This makes it feasible to use a highly resistive material such as maraging steel without precooling (which would not be efficient anyhow because the residual resistance of this material is large). These coils can be heated to much higher temperatures than it is admissible for copper coils, provided that temperature resistant insulating materials are used. However, even if these coils could be made strong enough to contain a megagauss field, the temperature would become excessive already in the vicinity of 80 T.

The Amsterdam magnet laboratory is the prototype for a facility that uses pulsed power directly from the mains. By contrast to a capitor discharge which results in a damped sine wave, the pulse shaping by controlled rectification of three phase current provides more flexibility. In any case, the field must be rapidly increased to its peak value such that the peak field is not limited by the resistance of the heated coil. The decrease of the field can then be programmed in a number of steps. The coil is cooled by liquid neon. With the given supply voltage, this results in a higher current because of the smaller resistance, but the lowered heat conductivity results in cooling times of the order of three hours. A typical cooling time for a liquid nitrogen cooled coil of average dimensions is 20 minutes.

Megagauss fields are characterized by the high energy density which becomes much larger than the energy density of chemical binding (as an example, take the heat of combustion of fossil fuels which is of the order of 40 kJ/cm^3). The effects of the high energy density come into play at the interface between the magnetic field and the conducting wall that confines the magnetic field. As the field increases, electromagnetic energy flows into the conductor at a

Table I. Computer simulation of wire-wound coils.

capacitor energy[a]	kJ	125					250			
wire cross section	mm^2	3				2	3			2
filling factor[b]		0.75				0.5	0.75			0.5
inner diameter	mm	16			20	16	20	16		20
outer diameter	mm	60					100	80		100
axial length	mm	80	100	150	100	100	100	100	160	100
peak field	T	62	56	46	52	50	47	58	47	41
rise time	ms	6.1	7.0	9.0	6.8	6.0	25	15.8	21.3	21
half period	ms	14.9	17.7	24.4	17.1	15.9	60	42 55		
temp. at peak	K	13	127	114	128	161	121	142	123	144
final temp.[c]	K	29	225	181	231	367	220	280	225	
homogeneity [d]	%	.87	.42	0.1	0.72	.42	I	.55	.12	
copper mass	kg	.41	1.76	2.64	1.68	1.17	5.05	3.23	5.17	3.37

a) charging voltage 5000 V
b) (copper volume) / (total volume)
c) with crowbar resistor 0.5 Ω
d) within a sphere touching the inner wall

rate given by the pointing vector

$$\vec{E} \times \vec{H} = v_f \mu_0 \cdot H^2 \qquad (2)$$

where $v_f = E/B$ is a speed that can be interpreted as describing the flow of magnetic flux in the direction perpendicular to the field lines. The form of eqn. (2) suggests that approximately one half of the energy is converted into Joule heat while the other half remains in the form of magnetic energy density $\mu_0 \cdot H^2/2$; this is true under the condition that the skin depth is small compared to the thickness of the conductor in the direction of the energy flow. The skin depth can be estimated by comparison to an exponential field rise which results in a field profile

$$B(x,t) = B_0 e^{\nu t} e^{-x/a} \text{ with } a = \sqrt{\frac{\rho}{\nu \mu_0}}. \qquad (3)$$

It turns out that in coils of practical size the skin depth is indeed smaller than the conductor thickness. As a consequence, the Joule heating becomes independent of the resistivity and depends only on the specific heat per volume (which is of the order 3 $J/(cm^3K)$ for most metals) and the square of the magnetic field. For example, the melting point of copper is reached at 110 T and the boiling point at 150 T. Beginning at the surface, the conductor will thus melt and vaporize at such a rate that it literally explodes. This explosion proceeds into the material at a speed of the order km/s which is related to the rate of energy input and the heat of vaporization (Bryant, 1966). This sets a limit to the duration of the field pulse but there is another effect which forces the pulse duration to be even shorter: the volume compression of the conductor material by the magnetic stress. Due to the rapid increase of the field already dictated by the Joule heating, the compression proceeds into the conductor material as a shock wave, and the wall recedes from the magnetic field at the speed of the medium (the "particle speed") behind the shock wave. The relations between particle speed, shock speed and pressure are well known as they represent the equation of state of the material: examples are given in Table III. It is evident that this effect provides a natural limit for the pulse duration of the order of a few microseconds or less. In practice, two methods are in use to generate megagauss fields for experimental applications: the direct discharge of electromagnetic energy into a small single turn coil and magnetic flux compression by the rapid implosion of a conducting shell. As primary energy sources, capacitor banks and high explosives have been used. Although high explosives are much more reliable and easier to use than most people would believe, the capacitor discharge is of course the preferred method for laboratory use. With single turn coils and a 40 kV, 100 kJ capac-

Table II. Presently operational pulsed field installations for nondestructive pulsed. fields

LABORATORY	max. field	i.d.	duration[a]	energy	voltage
		Controlled	*power*		
	T	mm	ms	kJ	kV
Amsterdam	40	20	1000/10	1500	0.66
Sendai	35	18	100/10	1400	0.35
M.I.T.	40	20	500/100[b]	1000	0.2(0.25[c])
		Capacitor	*banks*		
M.I.T.	50	20	10	100	4
Toulouse	40	26	400[d]	400	6
Toulouse	40	30	920[d]	1250	10
Osaka	60	20	0.37	490[e]	26.6[f]
Osaka	39	60	0.41	420[e]	26.6[f]
Tokyo	42	16	4	32	3.3
Tokyo	45	16	20	200	5-10
Leiden	52[g]	20	17	180	3
Braunschweig	27	13	150	40	2.5
Geneva	51[g]	14	15	72	2.5
Leuven	45	10	10	70	3.5
Moscow (Kurchatov)	50	20	15	190	5
Wroclaw	47	10	10	70	
Nijmegen	40	20	15	100	5
Vienna[h]	28			25	2.5
Poznan	92	6	1	427[i]	3/6

a) For controlled d.c. power, the total pulse duration and the duration of the flat top are given, for capacitor banks the half period of the sine wave.
b) Computer simulation
c) Capability of the power supply
d) "crowbar" waveform: the duration of the peak is smaller than in a sine wave
e) Total energy installed 1250 + 250 kJ
f) Convertible to 40 kV
g) These coils are reported to last only a few shots under favorable circumstances, typical performance is below 45 T, e.g. at Geneva 40 T with 36 ms pulse duration.
h) A magnet with pulsed power from the mains is under construction
i) Three separate capacitor banks for a three-layer polyhelix: 22.5 kJ at 3 kV, 135 and 270 kJ at 6 kV.

Table III. The surface speed of a compressible conductor subjected to a pulsed field (km/s)

Tesla	Al	Cu	Ta	Pt
100	0.25	0.11	0.07	0.05
500	3.55	1.71	1.22	0.92
1000	8.53	4.30	3.26	2.49

itor bank, 150 T have been reproducibly generated in 10 mm diameter with a rise time of 2 μs and 250 T in 4 mm diameter. In a single turn coil, the magnetic field protects the sample against destruction by the exploding conductor, while in an implosion system the sample is always destroyed by impact shortly after peak field. With explosive-driven flux compression, fields up to 1000 T have been generated for experimental applications (Pavlovskii et al., 1980).

It may appear difficult to do experiments in megagauss fields, and it certainly is! However, it has been demonstrated that suitable experimental

techniques can be developed and that resonance experiments in particular are well suited (Miura and Herlach, 1985). With megagauss fields, resonances are shifted into the range of 10 μm or smaller which is covered by the CO_2 and CO lasers. These experiments have been extended even into the temperature range of liquid helium. For most solid state experiments, it is indeed the combination of high fields and low temperatures which brings out the interesting effects.

There is one problem that must be given careful consideration in all pulsed field experiments. This is the heating of conducting samples by eddy currents. If the skin depth is large compared to the sample thickness, the Joule heating can be estimated by assuming a current distribution which is a linear function of the distance from the center of sample where the eddy current density is zero. The spatial average of Joule heating power per volume V is given by

$$\frac{1}{V}\frac{dW}{dt} = \frac{d^2}{12\rho}\left(\frac{dB}{dt}\right)^2 \qquad (4)$$

Where d is the sample thickness perpendicular to the field and ρ the resistivity. If the skin depth becomes small compared to the sample thickness, the heating is concentrated at the surface as it has been discussed for the coils, and in addition the sample is subjected to mechanical stress resulting from the magnetic stress (Maxwell tensor) which is converted into mechanical stress within the skin depth. For most experiments, a precise measurement of the magnetic field is required. This is an easy matter in a pulsed magnetic field: the voltage induced in a simple pick-up coil is exactly proportional to the derivative of the magnetic field. This can be integrated either electronically or numerically, or by a combination of both methods. This field measurement can be precisely calibrated by comparison to a resonance with a well known g-factor such as the electron spin resonance in DPPH (Herlach et al., 1983). This has a g-factor of 2.0037 and a linewidth of 30 mT at liquid helium temperature.

III. Sources and Detectors

Up into the sixties, the only practical source in the infrared was thermal radiation, and detectors were simply detectors of heat (bolometers). One method of obtaining monochromatic radiation was selective multiple reflection on certain crystals ("Reststrahlen"). This state of affairs was drastically changed with the invention of the first infrared lasers, resulting in a lively development of powerful experimental techniques which is still in full swing. Most research groups who use infrared radiation for their experiments therefore are actively engaged in the development of techniques for the generation and detection of infrared radiation. A most comprehensive source of information regarding all aspects of the generation, detection and application of far infrared radiation (FIR) is the series of books edited by Button (1979). In the following, we therefore give only a general review and refer to these books for detailed information and further references.

The first FIR line at 28 μm was discovered in 1962 in the He-Ne laser and further lines at 85 μm and 133 μm were discovered in 1964. In the same year, stimulated emission in water vapor was discovered. A breakthrough was achieved with the discovery of the 337 μm line in HCN by Gebbie and his collaborators. Compared to the water lines, this is a very strong one and easily gives a power of 50 mW; thus it is well suited for use in experiments. The typical HCN laser is a gas discharge tube several meters in length, filled with a mixture of methane and nitrogen at a pressure of 1.5 mbar. A gas discharge of the order 2 kV, 1 A is passed through this tube which simultaneously produces HCN molecules from the mixture and brings them to the excited state. Higher power has been achieved by different modes of pulsed operation.

The year 1970 is another milestone in the development of FIR sources, as Chang and Bridges discovered the optically pumped FIR laser. At present, a very large number of transitions in molecular gases are known that can be excited into laser action by the radiation from CO_2 lasers. For each transition, a specific and precise excitation frequency is required. The spectrum of the CO_2 laser consists of four branches centered at 10.6 ("P"), 10.2 ("R"), 9.6 ("P") and 9.25 ("R") μm; within each branch there is a number of sharp lines, regularly spaced at intervals of $0.01 - 0.02\mu$m. Table IV gives a selection of typical lines for general use together with their pumping frequencies. There are many more lines available in the range of 18.3 μm–2.65 mm but some of these require molecules with specific isotopes which may be quite expensive. A list of known transitions has been periodically updated and published by Knight (1982) at the National Physical

Table IV. FIR Laser transitions excited by CO_2 radiation (50W).

	wavelength (μm)	pump line	typical power (mW)
Methanol	1223	9P16	1.5
	699	9P34	5
	570	9P16	10
	469	10P38	0.3
	392	9P36	10
	369	9P16	10
	254	9P34	1
	170.6	9P36	10
	164.3	9P16	3
	118.8	9P36	30
	96	9R10	10
Methanol (deuterated)	330	9R3	3
	305.7	9R8	1
	295.8	9R8	1
	229	9P6	5
Formic Acid	744	9R24	1
	513	9R28	5
	432	9R20	10
	418	9R22	1.5
	405	9R18	3
	393	9R18	10
	311	10R22	1
Methyl Bromide	2632	10P10	?
	1965	10P28	0,5
	1673	10P4	2
	380	10R18	5
	353	9P18	2

Laboratory. The most commonly used molecules are methanol and formic acid, the strongest known line is at 118.8 μm from methanol with a rated power of 90 mW c.w. A typical power of the CO_2 pump laser is 50 W. The operation of an optically pumped laser is delicate and requires some experience as two laser cavities must simultaneously be kept in tune, and the stability of the FIR radiation depends on both the frequency and amplitude stability of the pump laser, in addition to the mechanical stability of the FIR cavity. Feedback circuits range from simple analog devices to sophisticated computer-controlled systems for overall stabilization. In some cases, the same pump line can excite different transitions and care must be taken to make sure which wavelength or combination of wavelengths is actually emitted. Nevertheless, due to the relatively high power and the large frequency range, the optically pumped FIR laser has become the standard laboratory instrument. Several models are offered by different companies, but many researchers prefer to buy only the CO_2 laser and build their own FIR cavities according to the needs of the experiment. For efficient coverage of the entire available spectrum of FIR lines, several cavities are indeed needed.

Among the other devices that are still in common use, carcinotrons and IMPATT diodes are worth mentioning. Carcinotrons are special electron

tubes of the travelling wave type. Thomson-CSF manufactures a series of carcinotrons with frequencies from 69 to 400 GHz, with output powers from 50 mW at 400 GHz to 15 W at 69 GHz. These are convenient sources of radiation at the disadvantage of high price as each carcinotron covers only a narrow frequency range (e.g. from 69 – 72 and 360 – 400 GHz). For full coverage of the entire frequency range, a dozen tubes is needed. IMPATT (IMPact Avalanche Transit Time) diodes are available with a power of the order 20 mW between 200 and 300 GHz, 1 W at 100 GHz and 5 W at 10 GHz. There is certainly still much room for further development of solid state devices of one type or the other to provide convenient sources of radiation for experiments in the far infrared.

For the transmission of FIR from the source to the sample and to the detector, neither tuned waveguides nor geometrical optics can be used. It is possible to obtain limited focusing by means of lenses (made e.g. from polyethylene) and spherical mirrors. This is called "Gaussian" optics because there are no sharp focal points but rather a concentration of radiation in the form of a Gaussian distribution. The most common and convenient method is the transport through round pipes with an inner reflecting (metallic) surface. The attenuation is mainly dependent on the diameter of the pipe. It is possible to reduce or expand the pipe diameter by conical sections with a small opening angle and to go around corners by placing a mirror at the intersection of two tubes. At the open end of such a light pipe, the radiation emerges of course in all directions and care must be taken to make sure how the sample is irradiated. One way of obtaining a well defined irradiation of the sample is the use of a "Von Ortenberg stripline". This is a narrow channel between parallel plates where one or both walls consist of sample surfaces. The radiation is lead into the stripline from a light pipe by means of a long conical section.

A survey on the different types of infrared detectors has been given by Blaney (1978). Some of the excellent traditional types of detectors such as the Golay cell cannot be used in pulsed field experiments because of their limited frequency response. Fast bolometers can be used in the millisecond range but will be marginal in most pulsed experiments. Mostly, photoconductive solid state devices are used as detectors in pulsed fields, using semiconductors such as Ge, InSb, GaAs and HgCdTe. According to the band structure and the frequency range to be detected, the photoconductive response can be brought about by different mechanisms. There are transitions across the band gap or from impurity levels to the conduction band, or the "heating" of electrons in the conduction band which changes their mobility. Most of these detectors operate with low noise at the temperature of liquid helium. The frequency range of the InSb hot electron detector can be shifted by means of a moderate magnetic field which results in increased sensitivity ("Putley detector"). Typical performance data for a number of detectors are given in Table V.

IV. Antiferromagnetic Resonance

High field AFMR using pulsed fields has been performed by Foner (1957) as early as 1957, a few years after the first reports on AFMR by Trounson et al. (1950) and the description of the molecular field theory by Kittel (1951). These first measurements of AFMR in MnF_2 in pulsed fields immediately demonstrated the power of the method: by extending the range of magnetic fields the internal fields in the sample could be studied much more accurately. The resonance equation, as obtained by Keffer and Kittel (1952) for uniaxial ferromagnets, can be written as:

$$\omega/\gamma = (2H_E H_A + (\alpha H_0/2)^2)^{1/2} \pm H_0(1-\alpha/2) \quad (5)$$

Where ω is the externally applied frequency, γ the gyromagnetic ratio, H_E the exchange field, H_A the anisotropy field; H_0 the external field in the direction of the c-axis, and α the ratio of parallel to perpendicular susceptibility; parallel and perpendicular are meant with respect to the c-axis of the crystal. α is usually very small so that the resonance condition can be approximated by:

$$\omega/\gamma \approx (2H_E H_A)^{1/2} \pm H_0 \quad (6)$$

$(2H_E H_A)^{1/2}$ is the zero-field resonance frequency in magnetic field units. For MnF_2 it is equal to 9.6 T at very low temperatures. It follows roughly a Brillouin curve as a function of temperature because H_E is almost independent of frequency and H_A is proportional to M_0^2, the square of the sublattice magnetization. Johnson and Nethercot (Johnson et al., 1956) had determined a few points on that Brillouin

Table V. Selected far infrared detectors with a response time less than 0.1 ms.

type	responsivity [V/W]	rise time [sec]	NEP[a] [W/Hz]	Temp. [K]	opt.[b] [μm]
pyroelectric					
DLATGS[c]	5×10^{3}	10^{-9}	5×10^{-10}	300	window[d]
rectifiers					
Be-InSb point contact	2×10^{1}		4×10^{-10}	300	337
GaAs Schottky diode	10^{1}		10^{-8}	300	496
superconducting Nb-Nb	10^{3}		10^{-12}	4.2	337
photoconductive					
Ge:Ga	8×10^{6}	10^{-7}	6×10^{-14}	4.2	100
Si:As	10^{3}	10^{-9}	10^{-11}	1.6	200
GaAs	10^{7}	10^{-8}	4×10^{-14}	4.2	280
InSb	2×10^{2}	10^{-7}	10^{-13}	4.2	1000

a) noise equivalent power
b) wavelength of optimal responsivity
c) deuterated L-alanine triglycine sulfate (Philips type P 1603)
d) mainly dependent on the window material

curve using resonances in zero external field at high frequencies, up to 213 GHz. The pulsed field apparatus of Foner allowed measurements in large H_0 fields and therefore the low frequency mode could be observed at 35 GHz and 70 GHz where ω_1 is determined from eqn. (5) using the minus sign. His data extended over a wide temperature range, from 4.2 K to 60 K, close to the Néel temperature T_N and accurate values of the low temperature limit of $(2H_EH_A)^{1/2}$and of T_N could be deduced. It was evident that high-field resonances could contribute much to the study of antiferromagnetic substances. However, it appeared immediately in the subsequent work of Foner and collaborators that severe limitations are encountered, due to a combination of stringent requirements for alignment of H_0 with the anisotropy axis and linewidth problems.

These limitations are reflected in the fact that all the AFMR that have been successfully studied up to now in pulsed fields were observed in relatively low fields. Three groups have been very active in pulsed field AFMR: Foner and collaborators at the Lincoln Laboratory and the National Magnet Laboratory at M.I.T., Date, Motokawa and collaborators at Osaka, and Ozhogin, Shapiro, Gurtovoi and collaborators at the Kurchatov Institute.

The AFMR research in Foner's group started with MnF_2 (Johnson et al., 1956) and continued with Cr_20_3 (Foner, 1959; Foner, 1963), $(Cr_203)_{1-x}$ $(Al_20_3)_x$ (Foner, 1961; Foner et al. 1962), α-Fe_20_3 (Williamson et al., 1964; Foner et al., 1965) and α-$(Cr_{1-f}Al_f)_2O_3$ (Artman et al., 1965).

A considerable amount of useful experimental data were collected in resonance field versus temperature curves at different frequencies; one typical example is shown in Figure 1.

In the uniaxial samples used for AFMR the sublattice magnetizations M_1 and M_2 are aligned with the anisotropy axis and with the external field; the sample is in the antiferromagnetic (AF) phase. The spin flop (SF) phase should be reached at higher values of the external field, as can be seen from the phase diagram of a uniaxial antiferromagnet in Figure 2, taken from Shapiro et al. (1970). In the spin flop mode just after the transition the sublattice magnetizations M_1 and M_2 are almost perpendicular to H_0. They gradually align with H_0 as the field is increased. This spin flop state is a consequence

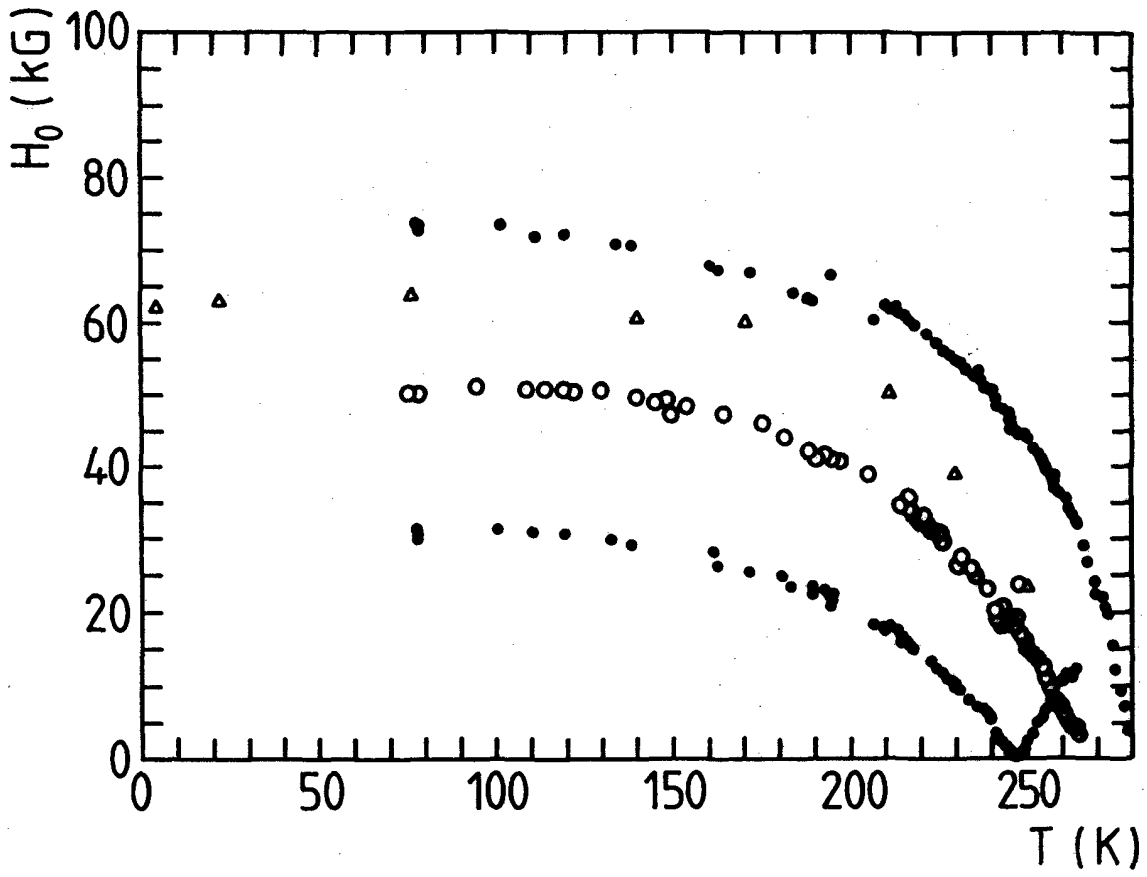

Figure 1. Antiferromagnetic resonance field H_0 vs temperature T in synthetic single crystal $\alpha-Fe_2O_3$ for H_0 parallel to the c axis. The closed and open circles correspond to 121 and 70 Gc/sec, respectively.

of the fact that the perpendicular susceptibility of a uniaxial ferromagnet is usually much larger than the parallel susceptibility such that the free energy can be lowered at some critical field by a transition to the perpendicular state.

Foner's work demonstrated that stringent limitations due to angular dependence of AFMR would impede observations of the spin flop mode: close to the spin flop field the required degree of alignment of the external field with respect to the c-axis of a unaxial crystal can be very high. It depends on the source frequency, as shown in Foner's application (Foner, 1963) of the general theory of Yosida (1952). The general conclusion is that high frequencies are needed to obtain observable spectra and that therefore far infrared sources should be combined with very high pulsed fields.

Motokawa and Date observed resonances in $CoCl_2 \cdot 2H_2O$ (Motokawa et al., 1965), $NiCl_2 \cdot 6H_2O$ (Date et al., 1967) and $MnCl_2 \cdot 2H_2O$ (Motokawa, 1978) and determined anisotropy constants and critical fields. Motokawa (1983) reports investigations in $MnFe_2.Rb_2$, MnF_4Cs, $MnCl_3 \cdot 2H_2O$ and Rb_2NiF_4. He tried to observe directly the transition from the spin flop state to the paramagnetic state by varying the temperature and the resonance field. However, line broadening prevented the observation of either the spin flop line or the paramagnetic line close to T_N. This broadening was due to a broad resonance background which occurs for large values of the magnetization, as explained in Section V.

Only in special types of antiferromagnetic materials like Cu-formate ($Cu(HCOO)_2 \cdot 4H_2O$) which is a kind of two-dimensional magnetic system, and TMMC which is one-dimensional, could the transition be observed (Motokawa, 1983) as a divergence

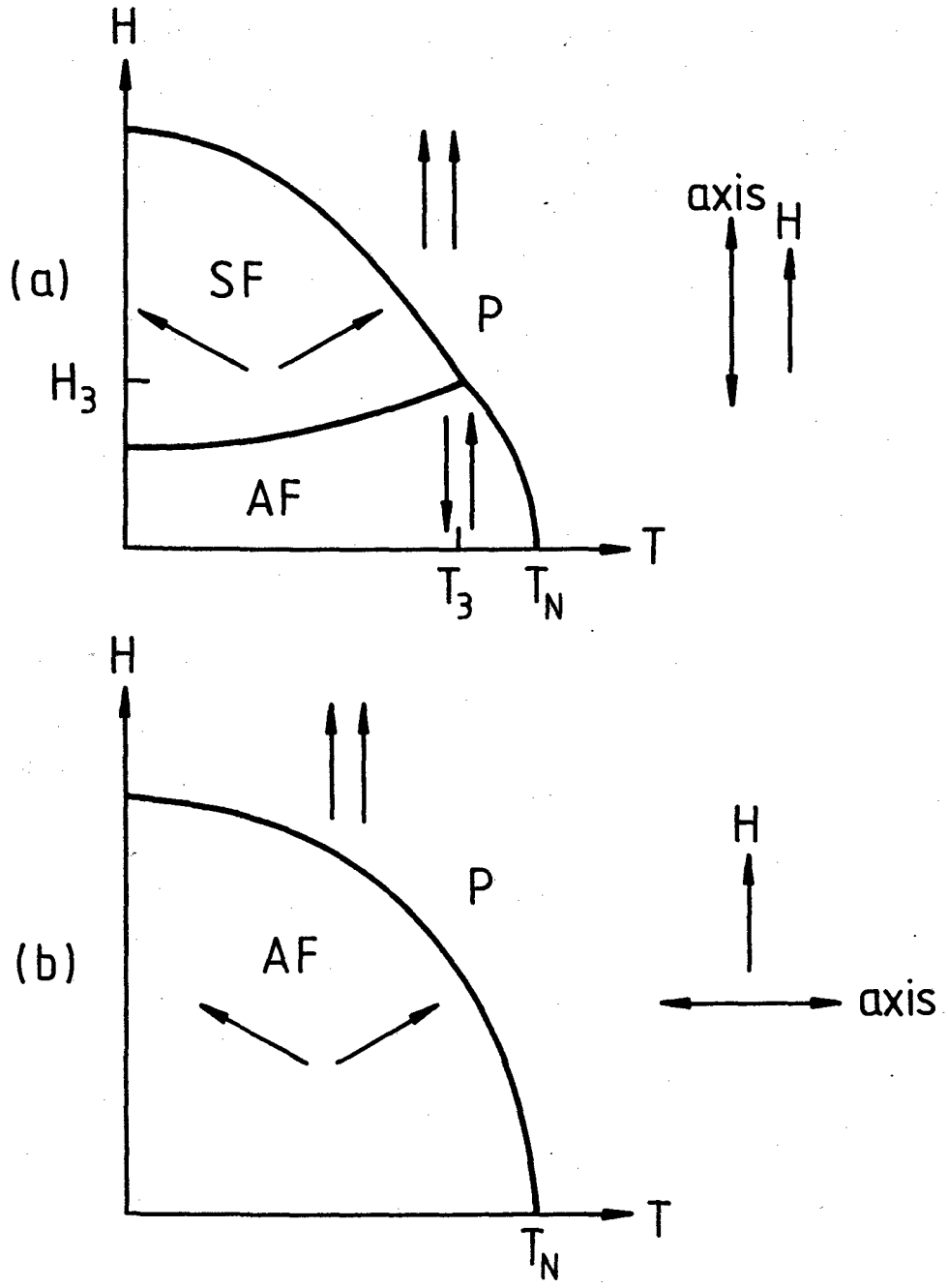

Figure 2. Schematic phase diagram for a uniaxial antiferromagnet, of the easy-axis type, with weak anisotropy: (a) H||n, (b) H⊥n. The arrows represent the magnetizations of the two sublattices.

of the linewidth.

Other techniques than ESR, like differential magnetization measurements (Shapiro et al., 1970) and magneto-optical absorption measurements (Caird et al., 1971) are more conveniently combined with pulsed fields to obtain magnetic phase diagrams.

At the Kurchatov Institute substances like α-Fe_2O_3 (Ozhogin et al., 1968; Ozhogin et al., 1969), CoF_2 (Gurtovoi, 1977; Gurtovoi, 1978), $YFeO_3$ and $SmFeO_3$ (Ozhogin et al., 1972) were investigated. Apart from the usual field-frequency and field-temperature relations (Gurtovoi et al., 1982) a thorough analysis of the Dzyaloshinskii (Dzyaloshinskii, 1958) interaction was given. Moriya (1960) showed

that this interaction is an anisotropic superexchange interaction proportional to the spin-orbit coupling. In its simplest form it contributes to the hamiltonian a term

$$-\beta(\vec{M}_1 + \vec{M}_2) \times (\vec{M}_1 - \vec{M}_2) \qquad (7)$$

where β is an interaction constant and $\vec{M}_1, \vec{M}_2$ are the sublattice magnetizations.

It gives rise to a so called Dzyaloshinskii field

$$H_D = 2\beta M_0$$

where M_0 is the magnitude of M_1 and M_2.

This field H_D enters in the expression for the resonance frequency and can therefore in principle be extracted from the resonance locus. However, its influence is only appreciable at high fields, because it enters into the resonance equations as a factor of H_0, the external field. In the work on α-Fe_2O_3 by Williamson and Foner (Williamson et al., 1964) H_D was found to be 2 T, whereas Ozhogin and Shapiro (Ozhogin et al., 1968) found 3 ± 0.4 T.

For CoF_2 a larger H_D field of 11.5 T was deduced from the resonance data by Ozhogin (Gurtovoi et al., 1982; Ozhogin, 1968). The phenomena that take place in CoF_2 at high fields parallel to the (001) axis were described by Gurtovoi et al. as follows: there are three critical fields: H_{c1}, H_{c2} and H_{c3}. In fields up to H_{c1} the magnetization vectors of both sublattices are antiparallel and the small difference in absolute value of the magnetic moments of the sublattices increases with increasing field. This difference is the cause of a relatively large susceptibility, even at very low temperatures. At H_{c1} a second order phase transition into an asymmetric canted phase takes place. When the field reaches H_{c2} a spin-flop state is established, in which both magnetization vectors have equal angles with the tetragonal (001) axis. Finally, at H_{c3}, a ferromagnetic phase is reached. The values of the transition fields are found to be:

$$H_{c1} = 21\text{T}; H_{c2} = 25.5\text{T}$$

H_{c3} could be estimated from a fitting procedure to be 75 T.

It appears from all these data that AFMR in pulsed fields has led to some interesting results but that many potential applications, especially for very high pulsed fields and very high frequencies, are still open.

V. EPR and FMR

The research groups mentioned in the previous section as active in AFMR research, have naturally also been involved in EPR work. Several special types of resonances, like impurity or spin- cluster resonances are equally related to AFMR as to EPR.

The first report on EPR in pulsed fields is again to be found in a publication by Foner (1959). In collaboration with Meyer and Kleiner (Foner et al., 1961) he studied EPR in 0_2 molecules trapped in single crystal β-quinol-chlatrate. These molecules have large zero-field splittings dependent on the interaction with nearest neighbors. Different nearest neighbor site occupation gave rise to a fine structure in the resonance data, with three different lines clearly resolved. This fine structure could be studied in detail with the pulsed field measurements, and a broad resonance absorption due to a $|\delta_M| = 2$ transition was found in addition. The measurement of zero-field splittings is evidently one of the first applications of EPR to be investigated in pulsed fields. Apart from the energy gap in antiferromagnets, described by Foner (1957), one has the large $D(S_z)^2$ term in the iron group and the large crystalline field splitting in the rare earth group. As an example the determination of the zero-field splitting of V^{3+} in Al_2O_3 by Foner (Foner et al., 1960; Foner, 1962) can be mentioned. A representative example of the iron group is Fe^{2+} in $CdPS_3$, investigated by Motokawa (1983). The experiment was done at a wavelength of 0.119 mm in a resonant field of 11 T, and the value of D deduced from the $|-1\rangle$ to $|-2\rangle$ transition was -24 cm^{-1}. Such a large splitting could only be observed in a laser spectrometer tuned to resonance by a large external field. Several impurity spin resonances in antiferromagnetic host materials were investigated by the Osaka group. Motokawa et al (1967) observed Fe^{3+} and Mn^{2+} resonances in $FeCl_2$, combining pulsed fields with several microwave frequencies at low temperatures. The important factor for the observation of those impurity resonances is the relatively weak exchange coupling between the impurity spin and the spin of the host material. From the resonance data the different effective interaction fields together with possible models for the impurity coordination were deduced. Analogous investigations were done by Fujii et al. (1968) for Mn^{2+} impurities in $CoCl_2 \cdot 2H_2O$. An interesting result was obtained by Date and Motokawa (Motokawa et al., 1965; Date

et al., 1966; Date et al., 1968) when they observed resonances in $CoCl_2.2H_2O$ which could not be interpreted as antiferro-, ferri- or ferromagnetic. The curious field-frequency and field-intensity relations for the different resonance branches that were observed could be explained satisfactorily by a spin-cluster resonance model. The spin structure of $CoCl_2 \cdot 2H_2O$ is a reasonably good approximation of an Ising spin chain because it consists of linear chains with strong ferromagnetic exchange, coupled by a weak antiferromagnetic exchange (Oguchi, 1965). In an Ising system a spin cluster state can be an eigenstate, where some neighboring spins have a direction opposite to that of the majority of spins in the chain, because there are no transverse components of spin. A spin cluster resonance involves the reversal of a terminal spin in the cluster and the resonance condition is, for an ideal Ising system, independent of either the exchange field HE or the anisotropy field H_A. Indeed, the spin reversal leaves the exchange and anisotropy energies unchanged. In $CoCl_2 \cdot 2H_2O$ the inter-chain exchange fields enter into the resonance condition which explains the different resonance branches mentioned above.

A combination of resonances in 3d- and rare earth elements was studied by Golovenchits and Sanina (1976) at the Ioffe Physico-technical Institute, when they observed mm-wave magnetic resonance spectra of $ErCrO_3$ in pulsed fields. The Er^{3+} gave EPR and the Cr subsystem AFMR spectra, from which the parameters of the Er-Cr interaction were determined.

ESR for $g \approx 2$ in pulsed fields at far infrared (FIR) frequencies has up to now been studied only by a very small number of research groups. It requires the combination of FIR lasers and pulsed magnets. The groups involved in this research are the Osaka Group with Date and Motokawa, the group of ISSP in Tokyo with Miura and the group at Leuven with the authors of this article. Kido and Miura studied the FIR resonance in ruby (Kido et al. 1982; Miura 1984). This experiment was aimed at confirming the fast response of the measuring system and to show the constancy of the g-factor up to very high fields and therefore to demonstrate the usefulness of ruby as a material for calibration of magnetic fields in the megagauss range. Date and coworkers produced an impressive number of excellent results using submillimeter ESR in pulsed fields. Their first paper on this subject (Date et al., 1975) reported on near-megagauss ESR in $CuCl_2 \cdot 2H_2O$. A multilayer coil (Date, 1975) had been designed to produce magnetic fields close to 100 T, and was therefore capable of producing the resonance field for a HCN laser. The exchange splitting, occurring whenever the external field exceeds the exchange field between dissimilar spins, was clearly observed as shown in Figure 3. A similar study was performed in CTS ($Cu(NH_3)_4 \cdot SO_4 \cdot H_2O$) (Date et al., 1975) in a slightly higher field up to 40 T. CTS was considered as an antiferromagnetic linear chain system and the intrachain exchange interaction was determined in this experiment. It came out to be much lower than had been anticipated, showing that CTS was not at all a good representative of linear chain systems.

In a general overview of the results obtained up to then, Motokawa et al. (1979) discussed the exchange splittings for ferro- and antiferromagnets with two unequal spins in the unit cell.

As shown in Figure 4 there are low field branches, ω_- in the ferromagnetic and ω_+ in the antiferromagnetic case. These are called "acoustic modes" and the remaining branches are the "optical modes", which have an energy gap at low fields. In $(NH_4)2CuCl_4 \cdot 2H_2O$ which is of the ferromagnetic interaction type, the splitting of the observed lines could be qualitatively explained by this simple molecular field model.

The Osaka group demonstrated that very high magnetic fields reveal higher order terms in the Hamiltonian that remain otherwise undetected. Using 337 μm radiation from an HCN laser and 111 μm radiation from an H_2O laser, resonances in Co tutton salt ($(NH_4)_2Co(SO_4)_2 \cdot 6H_2O$) were recorded in fields up to 40 T (Kuroda et al., 1978). The g-factor of Co tutton salt varies from $g = 3.06$ to $g = 6.45$ in low fields. In high fields a SH^3 term, the first correction to be added to the usual SH term in the effective spin Hamiltonian, becomes appreciable. This term could be clearly observed in this experiment. Recent experiments by the Osaka group include some resonances of impurities in magnetic materials. Katsumata et al. (1985) studied Fe^{2+} localized excitations in $Fe_{(1-x)}Co_xCl_2 \cdot 2H_2O$. The resonant transitions, in fields of 24.9 and 32.4 T, could be analyzed by a simple model describing the impurity spins as paramagnetic spins in the effective field arising from the impurity-host exchange interaction. Motokawa et al. (1985) reported on

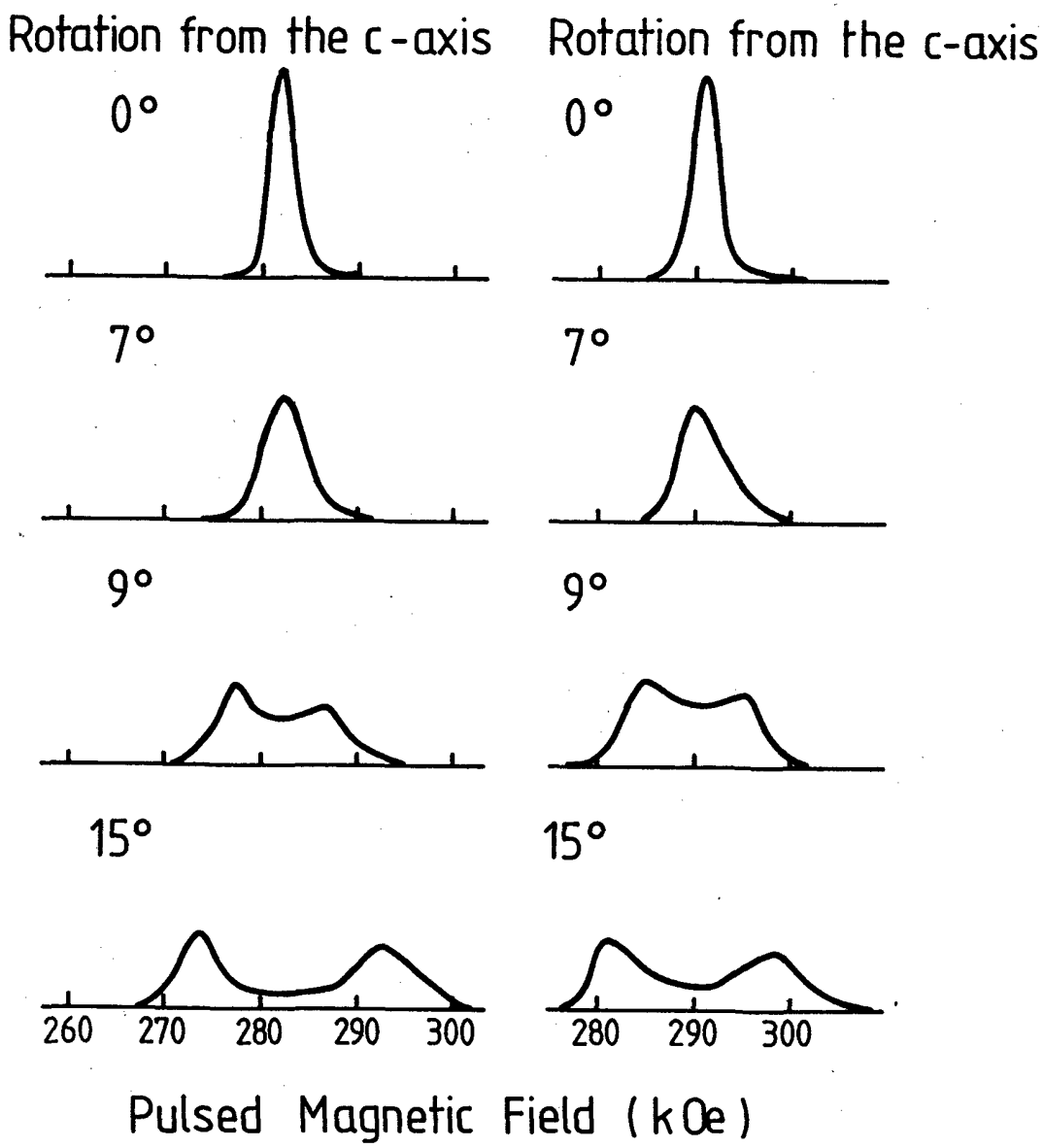

Figure 3. Line shapes of the resonances in $CuCl_2 \cdot 2H_2O$ in the ac-plane. Splitting of the lines due to two dissimilar spin systems is observed in strong magnetic fields. Along a- and c-axis the lines merge because these axes represent equivalent directions for the g-tensors.

sub-mm wave ESR of Mn^{2+} impurities in FeF_2 in pulsed fields up to 40 T. They observed linewidths varying with frequency, which could be explained by magnon-phonon interactions at neighboring Fe^{2+} spin sites to which the wavefunction of the Mn^{2+} spread out. An interesting material studied by the Osaka group as well as at Leuven is the well known tetramethyl ammonium trichloromanganate (TMMC) (De Groot et al., 1983; Motokawa et al., 1984; Motokawa et al., 1985). This substance is an example of an almost ideal quasi-one-dimensional Heisenberg spin system. The Mn atoms form linear chains; the exchange interaction in the chain is 6.5 K and the ratio with the interchain interaction is larger than 10^4. The g-shifts and linewidths could be measured in pulsed fields down to He temperatures at several FIR frequencies obtained from optically pumped far infrared lasers. Most experi-

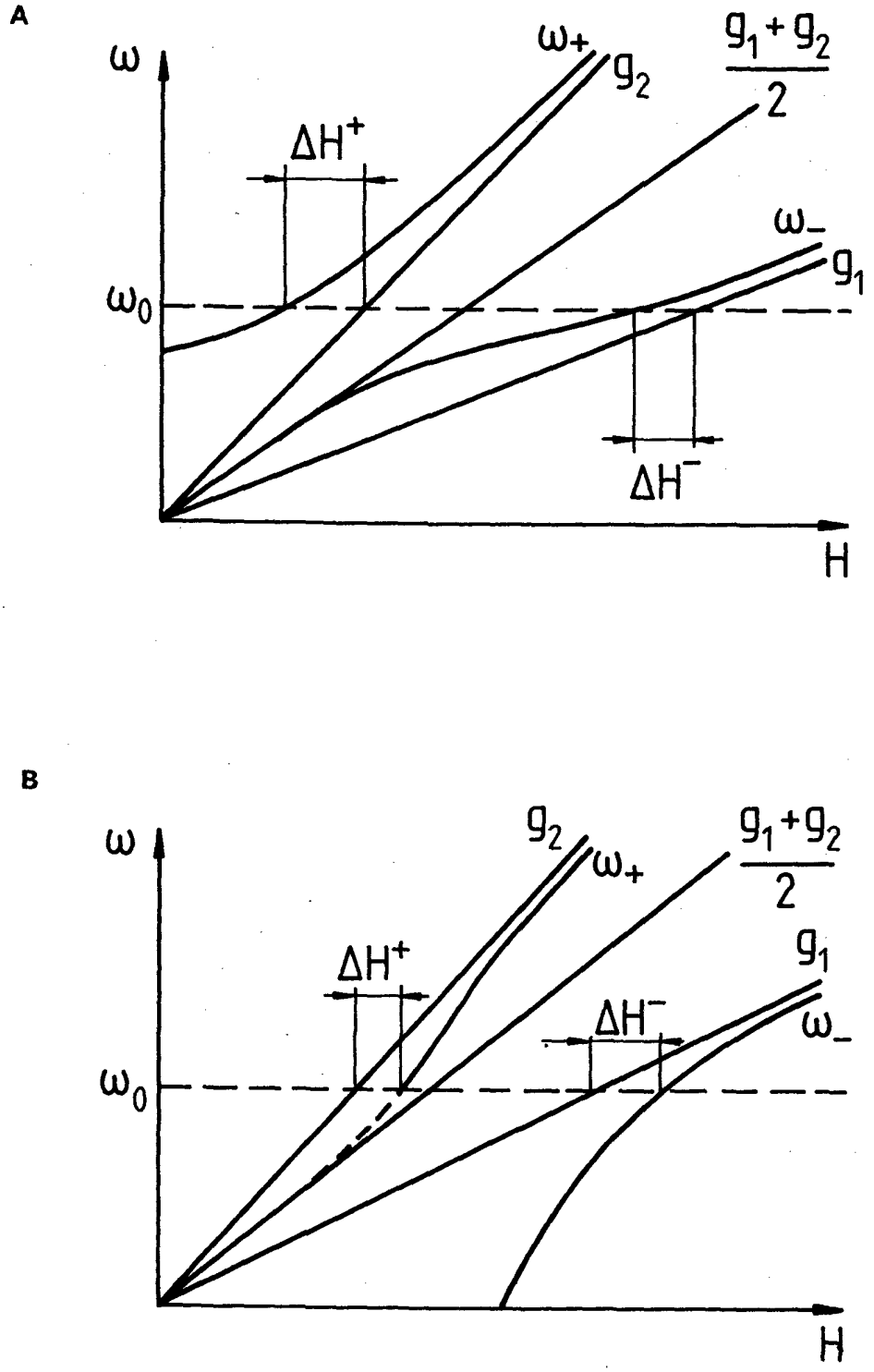

Figure 4. a) Schematic relation between ω and H for ferromagnetic interaction in a ferrimagnetic system with two spin sublattices characterized by g-factors g_1 and g_2. b) Schematic relation between ω and H for antiferromagnetic interaction.

mental data can be explained by a relatively simple model, regarding the resonance below about 10 K as AFMR-like and at high temperatures as paramagnetic. This is so because the resonance field is close to or exceeds the internal field responsible for the short range order in the system. However, at the highest frequency of 890.8 GHz the resonant field of 32.2 T is shifted from the field predicted by the

Table VI. Linewidths in Ni at 250 K versus resonance field.

Bres (T)	(GHz)	(μm)	B (T)
14.2	2689	699	1.39±0.05
17.5	3304	570	1.57±0.08
19.4	3669	513	1.63±0.03
22.9	4360	432	1.96±0.07
25.3	4794	393	2.08±0.05

model. Mechanisms like the Dzyaloshinskii Moryia interaction or soliton excitations may contribute to this shift but there is no quantitative explanation at present. At low temperatures a sharp peak in the linewidth is observed; this is supposedly connected to the Néel temperature. It is not certain that the temperature at which the linewidth is a maximum can be simply identified with T_N. This was done by Motokawa et al. (1984) and the result agreed well with a model based on soliton excitations by Harada et al. (1981). In the experiment of Motokawa et al. (1984) and in the model T_N was 3.5 K at a resonance field of 32.2 T. In the more recent experiments of Motokawa et al. (1985), however, the linewidth maxima were at 7 ± 1 K for a resonance field of 21 T and at 6 ± 1 K for 25 T. Combined with DC field measurements of Boucher et al. (1981), who found 3.4 K at 12 T, one would obtain an interesting and totally unexplained result of a T_N maximum at intermediate field strengths. But, as mentioned above, this depends on the identification of the linewidth-maximum with T_N which may be incorrect.

Finally, the first results of ferromagnetic resonance investigations in pulsed fields should be mentioned (De Groot et al., 1983). The general classical theory of FMR in metallic plates has been described among others by Wolfram and De Wames (1971). The complete theory of the power absorption by a metallic ferromagnet is rather complicated and has to be treated numerically. The essential features, however, can be demonstrated in a simple way, taking for example a plate perpendicular to the field, as follows:

Two waves with different k-vectors k_1 and k_2 enter the plate. k_1 determines the "skin"-wave; its properties depend on the conductivity of the medium i.e. on the skin effect. k_2 determines the "spin"-wave; it depends on the magnetization. Near resonance there is a strong interaction between the magnetization and the skin effect, through the h.f. susceptibility . Indeed, k_1 can be deduced from Maxwell's equations to be

$$k_1 = i\sigma\mu_0(1+\chi) \tag{8}$$

Now, if one calculates the resonant expression for χ from a Bloch-type equation, one obtains

$$\chi = \frac{\gamma M}{(-\omega + i\delta + \gamma(H-M) + i\sigma\mu_0 D)} \tag{9}$$

where ω is the frequency, γ the gyromagnetic ratio, H the static field, M the magnetization, σ the conductivity and D the exchange constant. The imaginary terms give the intrinsic (δ) and the exchange-conductivity ($\sigma\mu D$) contributions to the linewidth. For ferromagnets M can be much larger than these linewidth terms so that for $\omega = \gamma H$ the susceptibility is close to -1, which causes an anomalous transmission of the electromagnetic wave through the plate, called ferromagnetic antiresonance (FMAR). Between FMAR, with $\omega = H$ and FMR, with $\omega = (H - M)$ there is a forbidden transmission band with large values of χ. In this FMAR-FMR region one has therefore a broad resonance background, whose width is typically γM and has nothing to do with the intrinsic linewidth. The latter is clearly observed if standing spin waves form a discrete set of solutions governed mainly by the k_2 expression. In many cases only the lowest order spin wave mode can be observed and it merges with the FMAR to one complex line. The linewidth and g-factor then have to be extracted by computer simulations.

In Figure 5 some typical resonance lines for Ni are shown, for different FIR frequencies and resonance fields. The linewidths are given in Table VI. These linewidths are very large and increase linearly with frequency. In fact, they can be expressed as:

$$\delta = \frac{\omega\lambda}{\gamma M_s} + \delta$$

where δ contains the exchange-conductivity contribution to the linewidth, M_s is the saturation magnetization and λ is the so-called Landau-Lifshitz damping parameter. λ is found to be a constant. From microwave experiments (Hirst, 1965; Bhagat, 1966; Dewar, 1977) λ is determined to be about $(2.4 \pm 0.1)10^8\ s^{-1}$ at 300 K.

The FIR results give exactly the same value for λ. It is therefore well established that the linewidth

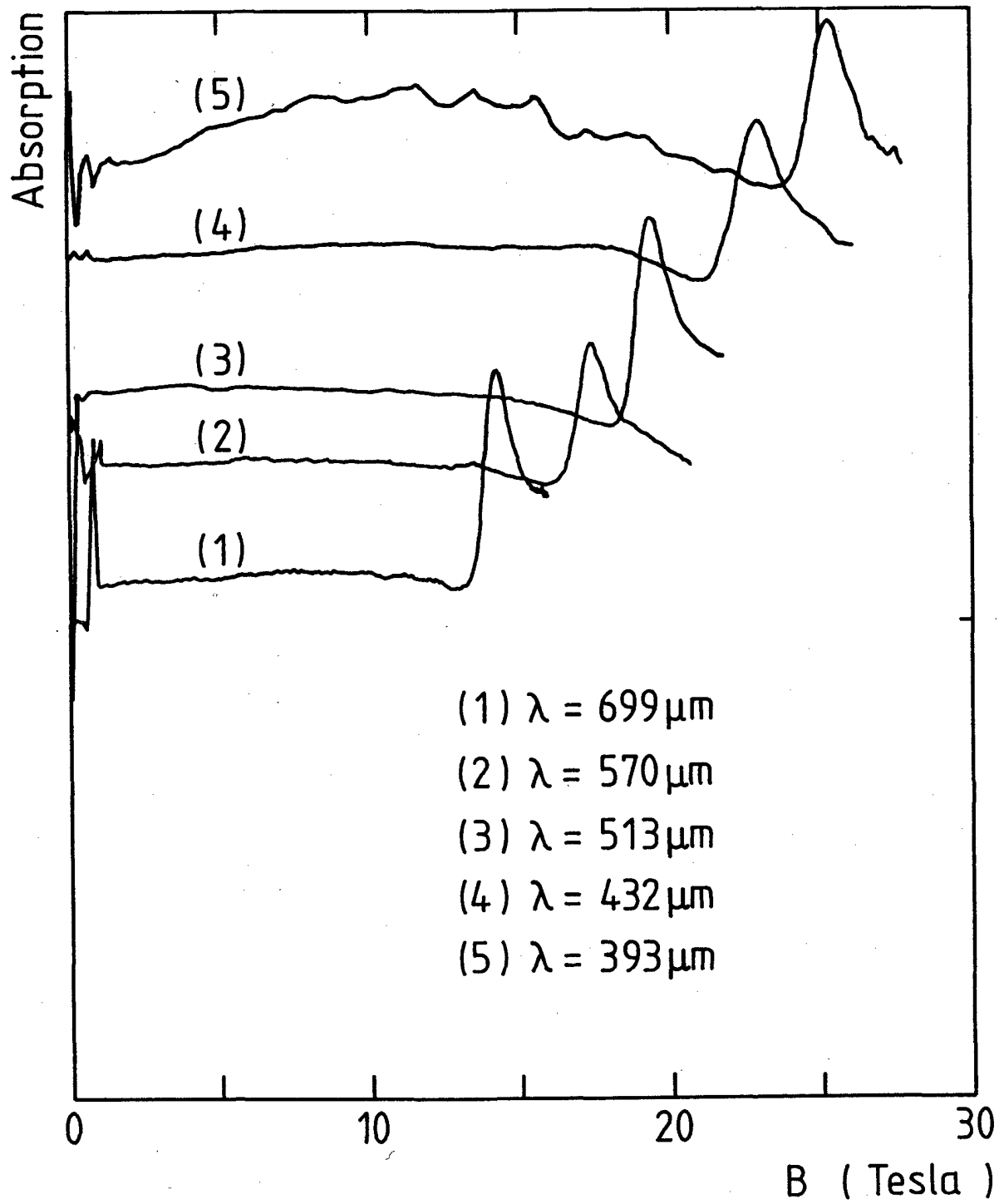

Figure 5. Ferromagnetic resonance lines in Ni for different far infrared frequencies. The wavelengths are (1) 699 μm (2) 570 μm (3) 513 μm (4) 432 μm (5) 393 μm.

in Ni, and also in other metallic ferromagnets, contains a term which is linear in frequency. A possible explanation, based on scattering of conducting electrons by phonons, combined with spin-orbit interactions, has been given by Kambersky (1970) but the exact magnitudes and temperature dependences are not predicted by that model. This remains an interesting problem for future research, as do indeed

many of the other topics mentioned in this review.

Acknowledgement

We greatly appreciate the help of L. Van Bockstal in preparing the manuscript.

VI. References

Artman, J.O., Murphy, J.C. and Foner, S. 1965, *J. Appl. Phys.* **36**, 986.

Askenazy, S. 1978, Proc. Conf., *The Application of High Magnetic Fields in Semiconductor Physics*, Oxford, Sept., 11-15, p. 101.

Bhagat, S.M. and Hirst, L.L. 1966, *Phys. Rev.* **151**, 401.

Blaney, T.G. 1978, *J. Phys. E: Sci. Instrum.* **11**, 856.

Boucher, J.F., Renault, L.P., Rossat-Mignod, J., Renard, J.P., Bouillot, J. and Stirling, W.G. 1981, *J. Appl. Phys.* **52**, 1956.

Bryant, A.R. 1966, in *Proc. Conf. Megagauss Magnetic Field Generation by Explosives and Related Experiments*, Knoepfel, H. and Herlach, F., Eds., Frascati 1965, (EURATOM Brussels), p. 183.

Button, K.J. 1979-1982, *Infrared and Millimeter Waves*, Academic Press, New York, pp. 1-6.

Caird, R.S., Garn, W.B., Fowler, C.M. and Thomson, D.B. 1971, *J. Appl. Phys.* **42**, 1651.

Chikazumi, S. and Miura, N. 1981, *Physics in High Magnetic Fields*, Springer Berlin-Heidelberg-New York

Date, M. and Motokawa, M. 1966, *Phys. Rev. Letters* **16**, 1111.

Date, M. and Motokawa, M. 1967, *J. Phys. Soc. Japan* **22**, 165.

Date, M. and Motokawa, M. 1968, *J. Phys. Soc. Japan* **24**, 41.

Date, M. 1975, *J. Phys. Soc. Japan* **39**, 892.

Date, M., Motokawa, M., Seki, A., Kuroda, S., Matsui, K., Nakazato, H. and Mollymoto, H. 1975, *J. Phys. Soc. Japan* **39**, 898.

Date, M., Motokawa, M., Hori, H., Kuroda, S. and Matsui, K. 1975, *J. Phys. Soc. Japan* **39**, 257.

Date, M. 1976, *IEEE Trans. Magn. MAG* **12**, 1024.

Date, M. 1983, *High Field Magnetism, Proc. Intern. Symp. on High Field Magn.*, Osaka 1982, North Holland, Amsterdam.

De Groot, P., Janssen, P., Herlach, F., De Vos, G. and Witters, J. 1983, *J. Magnetism and Magn. Mat.* **31-34**, 637.

De Groot, P., Janssen, P., Herlach, F., De Vos, G. and Witters, J. 1983, *Bull. Magn. Reson.* **5**,187.

De Groot, P., Janssen, P., Herlach, F., De Vos, G. and Witters, J. 1983, *High Field Magnetism*, M. Date, Ed., North Holland Publ. Co., p. 245.

Dewar, G., Heinrich, B. and Cochran, J.F. 1977, *Can. J. Phys.* **55**, 821.

Dzyaloshinskii, I. 1958, *Phys. Chem. Sol.* **4**, 241.

Fisher, F. 1975, *Proc. Conf. Phys. sous Champs Magnétiques Intenses*, Grenoble, Sept. 1974 (CNRS Paris 1975), 18-20, p. 79.

Foner, S. 1957, *Phys. Rev.* **82**, 565.

Foner, S. 1959, *J. Phys. Radium* **20**, 336.

Foner, S. and Low, W. 1960, *Phys. Rev.* **120**, 1585.

Foner, S. 1961, *J. Appl. Phys. Suppl.* **32**, 63S.

Foner, S., Meyer, H. and Kleiner, W.H. 1961, *J. Phys. Chem. Sol* **18**, 273.

Foner, S. 1962, *J. Phys. Soc. Japan* **17**, Suppl. B1, 424.

Foner, S. and Hou, S.L. 1962, *J. Appl. Phys.* **33**, 1289.

Foner, S. 1963, *Phys. Rev.* **130**, 183.

Foner, S. and Williamson, S.J. 1965, *J. Appl. Phys.* **36**, 1154.

Foner, S. 1967, *Proc. Conf. les Champs Magnétiques Intenses, leur Production et Leurs Applications*, Grenoble, Sept. 1966 (CNRS Paris 1967), 12-14, p. 385.

Foner, S. 1986, private communication.

Fujii, N., Motokawa, M. and Date, M. 1968, *J. Phys. Soc. Japan* **25**, 700.

Gersdorf, R., Müller, F.A. and Roeland, L.W. 1965, *Rev. Sci. Instr.* **36**, 1100.

Golovenchits, E.I. and Sanina, V.A. 1976, *Sovj. Phys. JETP* **42**, 665.

Gurtovoi, K.G. 1977, *Sovj. Phys. Sol. St.* **19**, 377.

Gurtovoi, K.G. 1978, *Sovj. Phys. Sol. St.* **20**, 1539.

Gurtovoi, K.G., Lagutin, A.S. and Ozhogin, V.I. 1982, *Sovj. Phys. JETP* **56**, 1122.

Harada, I., Sasaki, K. and Shiba, H. 1981, *Sol. St. Comm.* **40**, 29.

Herlach, F., De Groot, P., Janssen, P., De Vos, G. and Witters, J. 1983, *High Field Magnetism*, M.

Date, Ed., 1983, 229.

Herlach, F., De Vos, G. and Witters, J. 1984, *J. Phys., Proc. 8th Int. Conf. on Magnet Technology* 1983, **45**, Suppl. C1-915.

Herlach, F. 1985, *Strong and Ultrastrong Magnetic Fields and Their Applictions*, Springer Topic in Appl. Phys., **57**, Springer, Berlin-Heidelberg.

Hirst, L.L. and Prange, R.E. 1965, *Phys. Rev.* **139**, A892.

Hiruma, K., Kido, G. and Miura, N. 1979, *Sol. St. Comm.* **31**, 1019.

Johnson, F.M. and Nethercot, A.H. 1956, *Phys. Rev.* **104**, 847.

Kambersky, V. 1970, *Can. J. Phys.* **48**, 2906.

Kamigaki, K., Hoshi, A., Fuse, M., Ohashi, M. and Kaneko, T. 1979, *J. Magn. and Magn. Mater.* **11**, 328.

Katsumata, K., Uyeda, C. Motokawa, M. and Date, M. 1985, *J. Phys. Soc. Japan* **54**, 1244.

Keffer, F. and Kittel, C. 1952, *Phys. Rev.* **85**, 329.

Kido, G. and Miura, N. 1982, *Appl. Phys. Lett.* **41**, 569.

Kittel, C. 1951, *Phys. Rev.* **82**, 565.

Knight, D.J.E. 1982, *NPL report QU 45 (National Physical Laboratory,* Teddington, Middlesex TW11 OLW).

Knoepfel, H. and Herlach, F. 1966, *Proc. Conf. Megagauss Magnetic Field Generation by Explosives and Related Experiments*, Frascati 1965 (EURATOM Brussels).

Kuroda, S., Motokawa, M. and Date, M. 1978, *J. Phys. Soc. Japan* **44**, 1797.

Lira, J.A., Boon, W., Herlach, F., Janssens, L. and Kuppens, J. 1975, *Proc. 5th Int. Conf. on Magnet Technology*, Frascati 21-25, April 1975 (CNEN, Roma 1975), p. 264.

Miura, N, Kido, G., Miyajima, H., Nakao, K. and Chikazumi, S. 1981, *Phys. in High Magnetic Fields*, S. Chikazumi and N. Miura, Eds., Springer Berlin-Heidelberg-New York.

Miura, N. 1984, *Infrared and mm Waves*, F. Button, Ed., Academic Press, p. 12.

Miura, N. and Herlach, F. 1985, *Strong and Ultrastrong Magnetic Fields and Their Applictions*, Springer Topic in Appl. Phys., **57**, Springer, Berlin-Heidelberg, Chapter 6.

Moriya, T. 1960, *Phys. Rev.* **120**, 91.

Motokawa, M. and Date, M. 1965, *J. Phys. Soc. Japan* **20**, 465.

Motokawa, M. and Date, M. 1967, *J. Phys. Soc. Japan* **23**, 1216.

Motokawa, M. 1978, *J. Phys. Soc. Japan* **45**, 1528.

Motokawa, M., Kuroda, S. and Date, M. 1979, *J. Appl. Phys.* **50**, 7762.

Motokawa, M. 1983, *High Field Magnetism*, M. Date, Ed., p. 219.

Motokawa, M., Otsuka, A., Uyeda, C. and Date, M. 1984, *J. Phys. Soc. Japan* **53**, 1857.

Motokawa, M., Uyeda, C., Otsuka, A., Date, M. and Toussaint, R.M. 1985, *J. Phys. Soc. Japan* **54**, 2317.

Motokawa, M., Van Bockstal, L. and Herlach, F. 1985, *J. Phys. C. Sol. State Phys.* **18**, 5009.

Oguchi, T. 1965, *J. Phys. Soc. Japan* **20**, 2236.

Ozhogin, V.I. 1968, *J. Appl. Phys.* **39**, 1029

Ozhogin, V.I. and Shapiro, V.G. 1968, *Sovj. Phys. JETP* **27**, 54.

Ozhogin, V.I. and Shapiro, V.G. 1969, *Sovj. Phys. JETP* **28**, 915.

Ozhogin, V.I., Shapiro, V.G., Gurtovoi, K.G., Galst'yan, E.A. and Chervonenkis, A.Ya. 1972, *Sovj. Phys. JETP* **35**, 1162.

Ozhogin, V.I., Gurtovoi, K.G. and Lagutin, A.S. 1983, *High Field Magnetism*, M. Date, Ed., North Holland, Amsterdam 1983, p. 267.

Pavlovskii, A.I., Kolokolchikov, N.P., Tatsenko, O.M., Bykov, A.I., Dolotenko, M.I. and Karpikov, A.A. 1980, in *Megagauss Physics and Technology.*

Praddaude, H.C. and Foner, S. 1979, *Rev. Sci. Instr.* **10**, 1183.

Schneider, D. and Salge, J. 1971, *Z. Ang. Phys.* **31**, 346.

Shapiro, Y. and Foner, S. 1970, *Phys. Rev. B1* **7**, 3083.

Trounson, E.P., Bleil, D.F., Wangsness, R.K. and Maxwell, L.R. 1950, *Phys. Rev.* **79**, 542.

Van Deursen, A.P.J., Buiting, J.J.M., Weger, M. and Moses, D. 1984, *J. Phys.* **F14**, L101.

Williamson, S.J. and Foner, S. 1964, *Phys. Rev.* **136**, 4A, A 1102.

Witters, J. and Herlach, F. 1983, *J. Phys.* **D16**, 255.

Wolfram, T. and De Wames, R.E. 1971, *Phys. Rev.* **B4**, 3125.

Yosida, K. 1952, *Progr. Theor. Phys. (Kyoto)* **7**, 425